30 Mar 2001

CFD Modeling of Multiphase Flow Distribution in Catalytic Packed Bed Reactors: Scale Down Issues

Y. Jiang

Mohan R. Khadilkar

Muthanna H. Al-Dahhan
Missouri University of Science and Technology, aldahhanm@mst.edu

Milorad P. Dudukovic

Recommended Citation

Y. Jiang et al., "CFD Modeling of Multiphase Flow Distribution in Catalytic Packed Bed Reactors: Scale Down Issues," *Catalysis Today*, vol. 66, no. 2 thru 4, pp. 209 - 218, Elsevier, Mar 2001.
The definitive version is available at https://doi.org/10.1016/S0920-5861(00)00642-8

ELSEVIER

Catalysis Today 66 (2001) 209–218

CATALYSIS TODAY

www.elsevier.com/locate/cattod

CFD modeling of multiphase flow distribution in catalytic packed bed reactors: scale down issues

Y. Jiang[1], Mohan R. Khadilkar[2], Muthanna H. Al-Dahhan, Milorad P. Dudukovic*

Chemical Reaction Engineering Laboratory (CREL), Department of Chemical Engineering, Washington University, St. Louis, MO 63130, USA

Abstract

Flow maldistribution in either a bench-scale or commercial scale packed bed is often responsible for the failure of the scale down unit to mimic the performance of the large reactor. The modeling of multiphase flow in a bench-scale unit is needed for proper interpretation of reaction rate data obtained in such units. Understanding the mechanism of flow maldistribution is the first step to avoiding it. In order to achieve this objective, computational fluid dynamic (CFD) simulations of multiphase flow under steady state and unsteady state conditions in bench-scale cylindrical and rectangular packed beds are presented for the first time. The porosity distribution in packed beds is implemented into CFD simulation by pseudo-randomly assigned cell porosity values within certain constraints. The flow simulation results provide valuable information on velocity, pressure, and phase holdup distribution.

Keywords: Catalytic packed bed; Multiphase flow maldistribution; Scaling down; Bench-scale; CFD simulation; Porosity distribution

1. Introduction

Packed bed reactors with multiphase flow have been used in a large number of processes in refinery, fine chemicals and biochemical operations. Effective scale up of bench-scale packed bed reactors in the development of new processes and scale down of the commercial units in the improvement of existing processes have become predominant tasks in the research and development divisions of many companies [1]. The paradigms of scaling up packed bed reactors from bench-scale to pilot scale and industrial units have been explored in detail in the literature [1–4] and reviewed recently by Sie and Krishna [1], Krishna and Sie [5], Dudukovic et al. [6]. The scaling down of multiphase packed bed is, in fact, even tougher since many issues such as liquid back mixing and liquid maldistribution become more apparent when the reactor scale is reduced [7,8]. The critical question is how to effectively produce reliable bench-scale data. To answer this question, and to come up with a new strategy for scaling down packed beds, studies of the following issues are required: (1) understanding multiphase flow maldistribution in bench- and pilot-scale packed beds, (2) assessing the effect of flow maldistribution on reactor performance in terms of conversion and selectivity; developing a method to 'correct' the bench- and pilot-scale experimental data for non-ideal flow behavior and (3) preventing flow maldistribution happening in experimental units (e.g., using fines [9,10]). In this paper, we mainly focus on the first aspect, which is

* Corresponding author. Tel.: +1-314-935-6021; fax: +1-314-935-4832.
E-mail address: dudu@poly1.che.wustl.edu (M.P. Dudukovic).
[1] Present address: Conoco Inc., 1000 South Pine St., Research west 6685, OK 74602, USA.
[2] Present address: GE Plastics, 1 Lexan lane Mt. Vernon, IN 47620, USA.

0920-5861/01/$ – see front matter
PII: S0920-5861(00)00642-8

Nomenclature

A_{gl}, A_{kl}	working parameters
B_{gl}, B_{kl}	working parameters
d_p	particle diameter (m)
E_1, E_2	Ergun constants ($E_1 = 180$, $E_2 = 1.8$)
f	particle external wetting factor
$F_{D(k-l)}$	drag between phases k and lg
g	gravity (m/s^2)
J	J-function
P or p	pressure (N/m^3)
P_G	pressure in gas phase (N/m^3)
P_L	pressure in liquid phase (N/m^3)
r	radial position in cylindrical coordinate (m)
R	radius of packed beds (m)
t	time (s)
THE1–3	solid, liquid and gas volume fraction in CFDLIB data set
u_k	material k interstitial velocity (cm/s)
u'_k	fluctuating part of material k interstitial velocity (cm/s)
U_{g0}	gas feed superficial velocity (m/s)
U_{l0}	input interstitial velocity, $U_{l0}=U_0/\varepsilon_B$ (m/s)
V_2	interstitial liquid phase velocity in CFDLIB data (cm/s)
V_3	interstitial gas phase velocity in CFDLIB data (cm/s)
V_k	superficial velocity of fluid k (m/s)
V_r	relative superficial velocity between gas and liquid defined in Eq. (5d) (m/s)
V_z	axial velocity component (cm/s)
X_{kl}	momentum exchange coefficient between phases k and l
X, Y	X–Y rectangular coordinates, vertical direction (Y), horizontal direction (X)
Z	r–Z coordinates, axial coordinate (Z)

Greek letters

α_k	material indicator ($\alpha_k = 1$ if material k is present; $\alpha_k = 0$ otherwise)
$\varepsilon(r)$	longitudinal averaged porosity at radial position r
$\varepsilon(z)$	cross-section averaged porosity at position z
θ_k	material k volume fraction ($\theta_k = \langle\alpha_k\rangle$), $k = g, l, s$
μ_g	viscosity of gas phase (Pa s)
μ_k	viscosity of fluid k (Pa s)
ρ_g	density of gas phase (kg/m^3)
ρ_k	density of material k, $\rho_k \equiv \langle\alpha_k\rho_0\rangle$ (g/cm^3)
ρ_0	material density (kg/m^3)
σ_s	surface tension
$\langle\ \rangle$	ensemble-average
$\nabla\cdot$	divergence

to understand how multiphase flow is distributed spatially and temporally in packed bed reactors and how this affects the laboratory-scale experimental data.

The experimental studies of the flow pattern in packed beds have been conducted mostly for the system with 'saturated' single phase flow (e.g., gas flow or liquid upflow) using exit velocity measurements [11] and few non-invasive measurements [12,13]. Multiphase flow measurements in bench-scale packed beds have not been reported in the open literature although the recent high-resolution tomography techniques provide hopes in that direction [13–17]. Therefore, numerical simulation of multiphase flow in bench-scale packed beds is of significance in offering an improved understanding of such flows.

The performance of a packed bed is mainly dependent on the dynamic flow texture in the tortuous interstitial space and kinetic characteristics of the system. Dynamic multiphase flow modeling in such complex multi-dimensional space is a challenging task due to a number of issues involved. For instance, one has to find ways to deal with: (i) complex geometry of the voidage space; (ii) various scales of flow distribution (i.e. particle scale, cell scale and bed scale); (iii) complicated interactions between flowing phases and between fluids and the stationary catalyst particles. To overcome these complexities of the system, a variety of simplified phenomenological models have been developed in literature. The following approaches were suggested: (a) 'diffusion' model (see [18]); (b)

'sphere-pack' model (see [19]); (c) 'percolation' theory (see [20]); (d) 'porous media' method (see [21]); (e) 'energy minimization' approach [22–24]. Most of these models dealt with gas–liquid concurrent downflow in 2D rectangular packed beds with relatively large size of particles (3–6 mm) at steady state condition. The modeling of two-phase flow in a bench-scale cylindrical tube with typical particle size used in industry is simply not available. Although computational fluid dynamics (CFD) has been recently applied in case of gas flow in a single-tube fixed bed for heat transfer study [25], the diameters of the tube and the particles (e.g., 12 cm tube with 5 cm particles) used are completely different than those employed in the study of catalytic reactions.

In this paper, we present our recent numerical efforts on two-phase flow modeling in bench-scale cylindrical and rectangular packed beds using the CFD tool. The results are presented for operations at steady and unsteady state (e.g., periodic liquid feed), which have been previously examined in the studies of catalyst screening and reactor performance enhancements [26]. The effects on the experiments for flow of non-uniformity inside the packed beds were discussed. To explore the fluid dynamic mechanism for performance enhancement under periodic inflow mode, a comparison of flow distribution under steady state liquid feed and periodic liquid input in packed beds is given.

2. Flow domain and its description

The difficulties in modeling flow in catalytic packed beds are mainly due to the complex nature of the flow domain that is formed by passages around randomly packed particles. The structure of this interstitial space inside the packed bed is mainly determined by particle size (d_p), particle shape (ϕ), ratio of column diameter and particle diameter (D_r/d_p), and the packing method. Experimental measurement and computer simulation of porosity distribution in packed beds have been the subject of many investigations for a considerable period of time [27,28]. Although the detailed 3D porosity information can be achieved through computer simulation of random packing [28], an axisymmetric description of 2D porosity distribution, $\varepsilon(r, z)$, can be considered a good approximation in a certain sense. The longitudinally averaged radial porosity profile, $\varepsilon(r)$ was experimentally found to oscillate for a distance of 3–4 particle diameters from the wall, whereas the cross-sectional averaged porosity along the length of the bed, $\varepsilon(z)$, is distributed randomly [29]. For flow simulation purpose, in axisymmetric cylindrical coordinates (r–z) one can generate a 2D pseudo-random porosity distribution constrained by the mean porosity and the longitudinally averaged radial porosity profile (i.e., $\varepsilon(r)$). Fig. 1 shows such generated porosity distribution by displaying the porosity profiles $\varepsilon(r)$ and $\varepsilon(z)$. The dimension of the reactor in Fig. 1 is 22.5 cm in length and 2.4 cm in diameter. The spherical particles used are 1.5 mm in diameter. It is well known that for a given reactor, the radial porosity profile, $\varepsilon(r)$ is changed with the change in particle diameter, and the axial profile, $\varepsilon(z)$ varies with repacking [27], but the mean porosity retains the same value.

We also generated a 2D porosity distribution in X–Y coordinates for a bench-scale rectangular bed packed with 3 mm particles as used in our discrete cell model approach [23,24]. The inflow gas is distributed uniformly with given superficial velocity, whereas inflow liquid is treated as either in steady flow or in periodic flow with uniform or non-uniform distributors.

3. Ensemble-averaged *k*-fluid model

The ensemble-averaged Eulerian/Eulerian k-fluid model implemented via CFDLIB, developed by Los Alamos National Laboratory [29], is used as a transient multiphase flow simulation tool. The model has been adapted to the packed bed, and therefore, can handle gas and liquid concurrently flowing downwards with a stationary solid phase [23,30,31]. The detail descriptions of CFD modeling efforts and model applications in packed beds are available elsewhere [30]. Here we only provide the key flow equations and the closure laws for trickle-bed modeling as follows:

Equation of continuity:

$$\frac{\partial \rho_k}{\partial t} + \nabla \cdot \rho_k u_k = 0 \tag{1}$$

Equation of momentum:

$$\frac{\partial \rho_k u_k}{\partial t} + \nabla \cdot \rho_k u_k u_k = F_{D(k-l)} + \rho_k g + \theta_k \nabla p - \nabla \cdot \langle \alpha_k \rho_0 u_k' u_k' \rangle \tag{2}$$

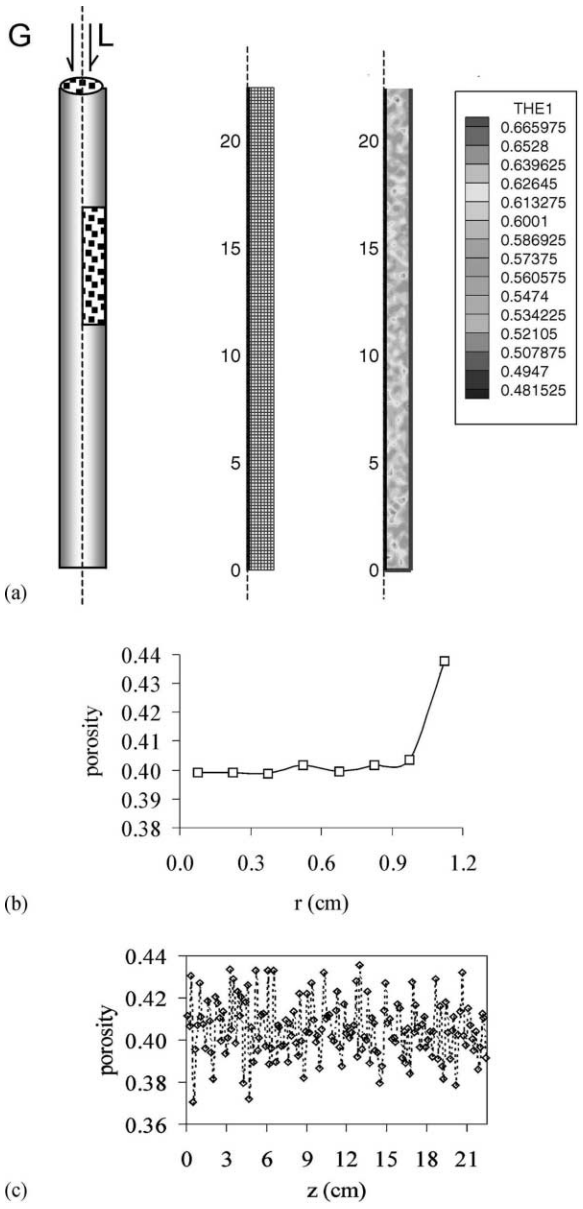

Fig. 1. Bench-scale cylindrical packed bed and its porosity description: (a) computer generated 2D axisymmetric solid volume fraction distribution; (b) radial porosity profile, $\varepsilon(r)$; (c) axial porosity profile, $\varepsilon(z)$.

The momentum exchange term, $F_{D(k-l)}$ is expressed as a product of the momentum exchange coefficient, phase volume fractions and relative velocity of the two phases k and l as below

$$F_{D(k-l)} = \theta_k \theta_l X_{kl}(u_k - u_l) \tag{3}$$

X_{kl} is calculated by the two-phase flow Ergun equation [31] in which constant Ergun parameters are used in this study ($E_1 = 180$, $E_2 = 1.8$). The effect of bed topology on Ergun parameters found in the bed scale phenomenological model [31] has been taken into account by the porosity distribution used in the flow distribution simulation. The exchange coefficient between liquid and solid phase (L–S) and gas and solid phase (G–S) can be written as

$$X_{ks} = (A_{ks}\mu_k V_k + B_{ks}\rho_k V_k^2)\frac{1}{\theta_s|u_k|} \tag{4a}$$

$$A_{ks} = 180\frac{{\theta_s}^2}{\theta_k^3 d_p^2} \tag{4b}$$

$$B_{ks} = 1.8\frac{\theta_s}{\theta_k^3 d_p} \tag{4c}$$

For gas–liquid drag, X_{gl} either no interaction is assumed for the low interaction regime [32] or the drag coefficient of two-fluid interaction model [33] is used

$$X_{gl} = \frac{\theta_g}{\varepsilon}(A_{gl}\mu_g V_r + B_{gl}\rho_g V_r^2)\frac{1}{\theta_l|u_g - u_l|} \tag{5a}$$

$$A_{gl} = 180\frac{(1-\theta_g)^2}{\theta_g^3 d_p^2}\left(\frac{\theta_s}{1-\theta_g}\right)^{2/3} \tag{5b}$$

$$B_{gl} = 1.8\frac{(1-\theta_g)}{\theta_g^3 d_p}\left(\frac{\theta_s}{1-\theta_g}\right)^{1/3} \tag{5c}$$

$$V_r = \theta_g|u_g - u_l| \tag{5d}$$

The influence of phasic pressure differences due to the interfacial tension and the gradient of liquid volume fraction, which reflects the contribution of capillary force on liquid flow distribution, is also taken into account in pressure calculations by Eq. (6). This equation was proposed by Grosser et al. [34] and modified by Jiang et al. [23] by introducing the particle wetting factor (f), which can be evaluated by the correlation of particle external wetting efficiency (see [35]).

$$p_L = p_G - (1-f)\frac{\theta_s E_1^{0.5}}{(1-\theta_s)d_p}\sigma_s \times \left[0.48 + 0.036\ln\left(\frac{1-\theta_s-\theta_L}{\theta_L}\right)\right] \tag{6}$$

The Reynolds stress term ($\nabla \cdot \langle \alpha_k \rho_0 u_k' u_k' \rangle$) is negligible in simulating macroscale flow although it may

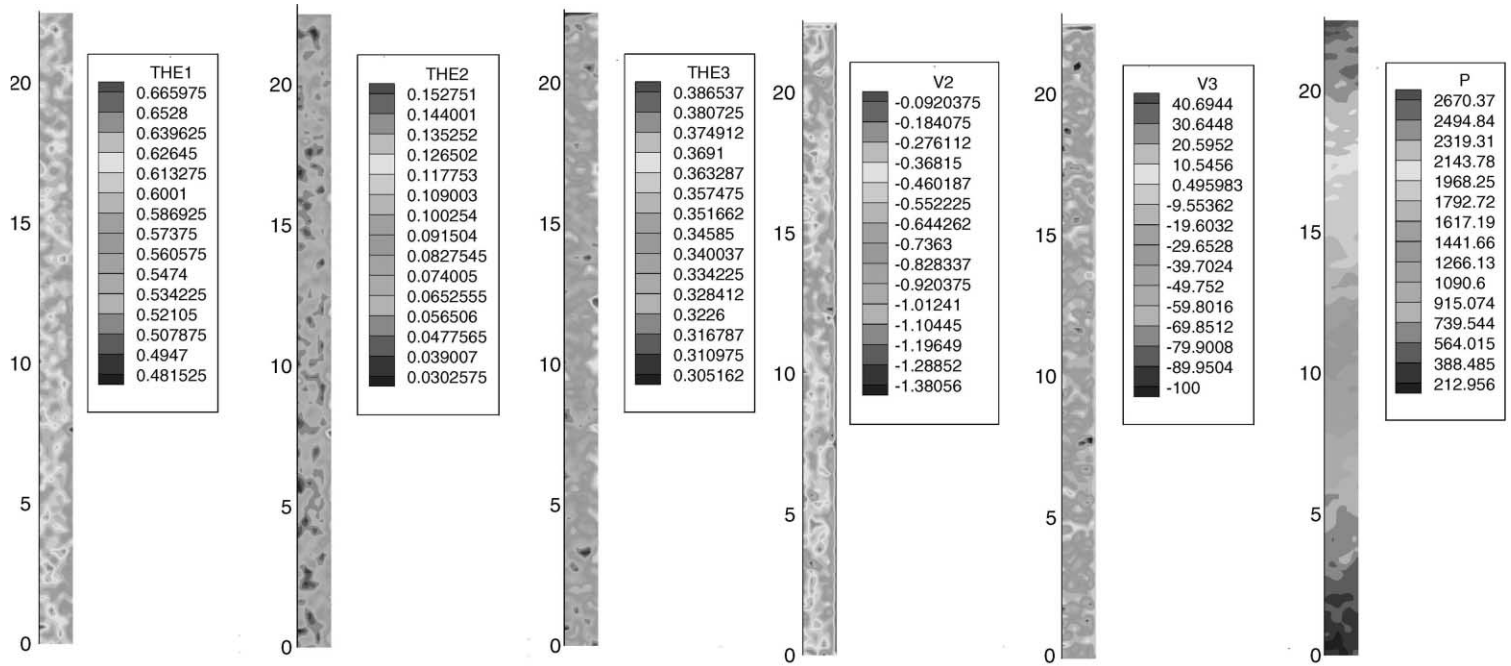

Fig. 2. Contours of packed bed structure and corresponded hydrodynamic parameters: (a) solid holdup: THE1; (b) liquid holdup: THE2; (c) gas holdup: THE3; (d) axial liquid interstitial velocity: V2; (e) axial gas interstitial velocity: V3; (f) pressure at $U_{g0} = 6\,\mathrm{cm/s}$ and $U_{l0} = 0.3\,\mathrm{m/s}$ at steady state operation.

be important for local scale flow modeling at high Reynolds number in packed beds [24].

4. Numerical simulation results and discussion

To demonstrate the capability of this model, we examined both the spatial distribution and the temporal phenomena associated with liquid flow at steady state and under periodic inflow conditions. Fig. 2 shows the spatial distributions of phase volume fraction, interstitial velocity and pressure at steady state inflow condition ($U_{g0} = 6\,\text{cm/s}$ and $U_{l0} = 0.3\,\text{cm/s}$). Higher liquid holdup (THE2) occurs in higher porosity zones (1.0-THE1) such as in the wall regions. Since local porosity value is changed by repacking the column even when using the same particles and procedure, it is clear that the point measurement of liquid–solid mass transfer coefficient $(ka)_{ls}$ using a conductivity method in repacked beds may result in a large scatter in data, which may lead to erroneous conclusions based on single point experiments [36]. Local measurement with a fixed structural matrix may give some meaningful data by a statistically generated set of large number of experimental conditions [37], which may be very time consuming. Since the radial component of velocity is relatively much smaller than the axial component and also normally distributed around the zero value, only the axial velocity component (V_z) is shown in Fig. 2 for the liquid (V_2) and the gas (V_3). Inspection of these figures indicate that, lower the porosity, lower the liquid holdup, and lower the liquid interstitial velocity. We do find some back flow of gas in Fig. 2(e), which is similar to the experimental findings for liquid upflow inside packed beds reported by Sederman et al. [13]. The negative local gas velocity leading to local counter-current flow of gas and liquid may explain why in the high interaction regime the slit model of Holub et al. [32] needed to be modified by Al-Dahhan et al. [38] to include a 'negative' slip between gas and liquid at the gas–liquid interface. More back mixing can be expected for gas flow in high pressure trickle-bed reactors due to the negligible gravity effect at elevated pressure. In general, pressure decreases along the bed axis (see Fig. 2(f)), however, relatively low pressure values occur at the wall region at each cross-section of the column due to higher porosity in proximity of the wall. This may cause errors in pressure measurement if one detects pressure just at the wall. Inserting multiple pressure sensors at different radial position is a way to avoid such errors; however, special care does need to be taken for the

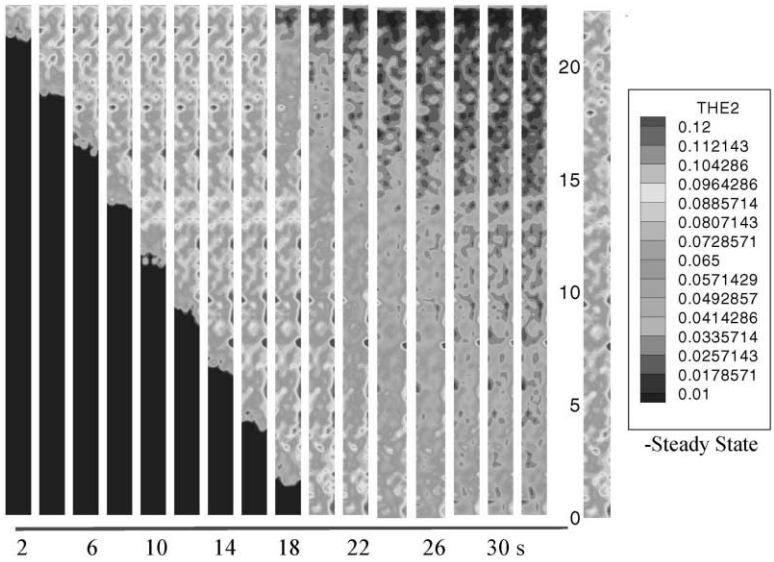

Fig. 3. Liquid holdup distribution in a periodic liquid inflow modal (15 s-on and 45 s-off) (left) and steady sate modal (right) in 1 in. cylindrical packed bed at $U_{g0} = 6\,\text{cm/s}$ and $U_{l0} = 0.3\,\text{cm/s}$.

disturbance that the sensors can cause in the local flow distribution.

The temporal phenomena of liquid flow are shown in Fig. 3 in a 1 in. cylindrical tube with uniform gas inflow but with a periodic liquid inflow (60 s cycle time = 15 s turn-on + 45 s turn-off as used in reaction studies of Lange et al. [39], Castellari and Haure [40], Khadilkar et al. [26]). Since the axisymmetric

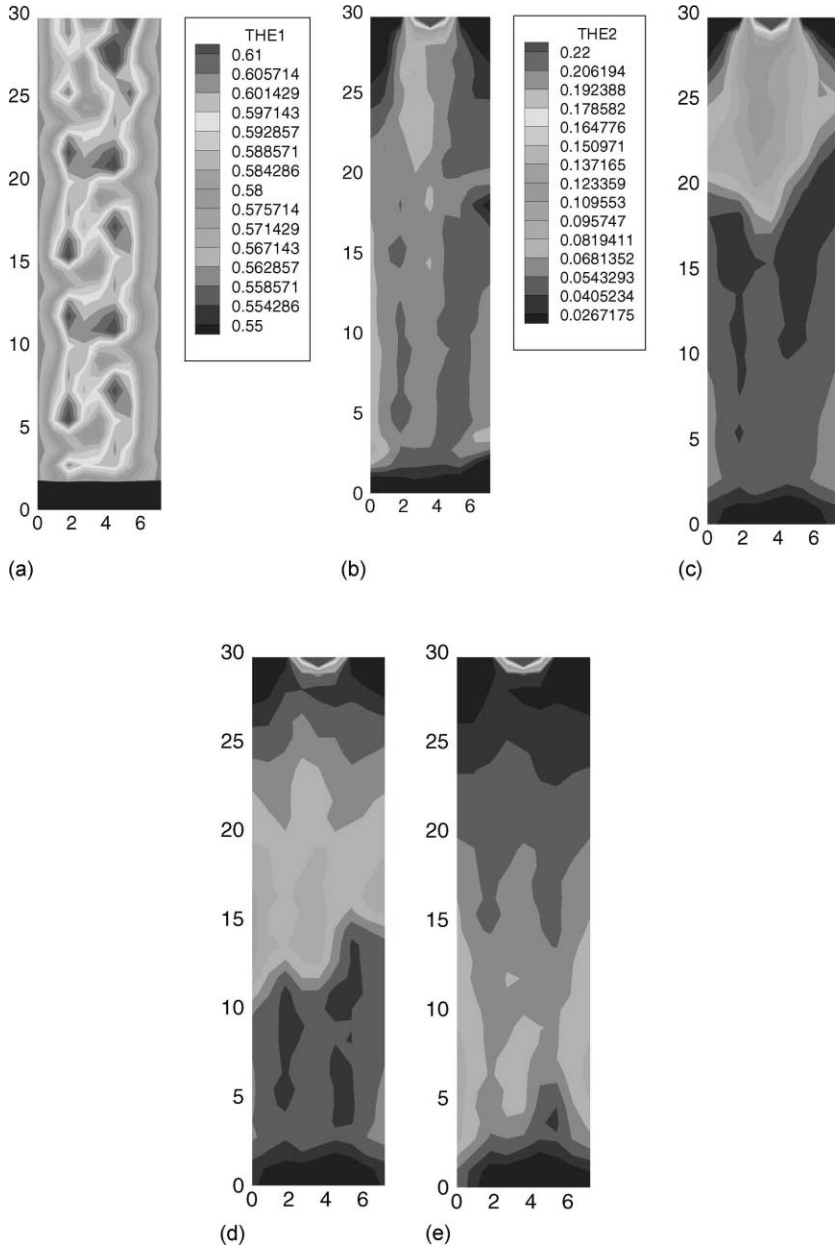

Fig. 4. (a) Solid holdup (THE1 = 1.0-bed porosity) distribution in the model 2D rectangular bed. Snapshot of liquid holdup (THE2) contours at (b) steady state liquid feed; (c) $t = 15$ s; (d) $t = 25$ s; (e) $t = 40$ s from start of the liquid ON cycle (left) in comparison with steady state holdup contours (right).

assumption is used in the simulation, there is no way to catch all the real time scales of the flow, but we are able to look at the time scale in the axial direction due to the dominant velocity component (V_z). It is found that the simulated liquid flow readily reaches the steady state values because the fluid cannot flow azimuthally. Once the front of the liquid stream reaches the bottom of the packed bed, the flow field is developed as shown in Fig. 3. The liquid draining from the bed takes time and certain amount of liquid still stays in the bed even after another 15 s.

A test case with a possibility of significant liquid maldistribution was chosen for investigating the effects of induced liquid flow modulation. A 2D rectangular model bed of dimensions 29.7 cm × 7.2 cm was considered with pre-assigned porosity values to different cells (33 in the vertical (Y) direction and 8 in the horizontal (X) direction as shown in Fig. 4a). Liquid flow was introduced at the two central cells at the top of the bed at mean superficial velocity of 0.1 cm/s, while gas flow was introduced in the rest of the cells at a superficial velocity of 10.0 cm/s in simulations of both steady and unsteady state operation. Steady state simulations show evidence of significant liquid maldistribution, particularly at the top and bottom of the reactor. Complete absence of

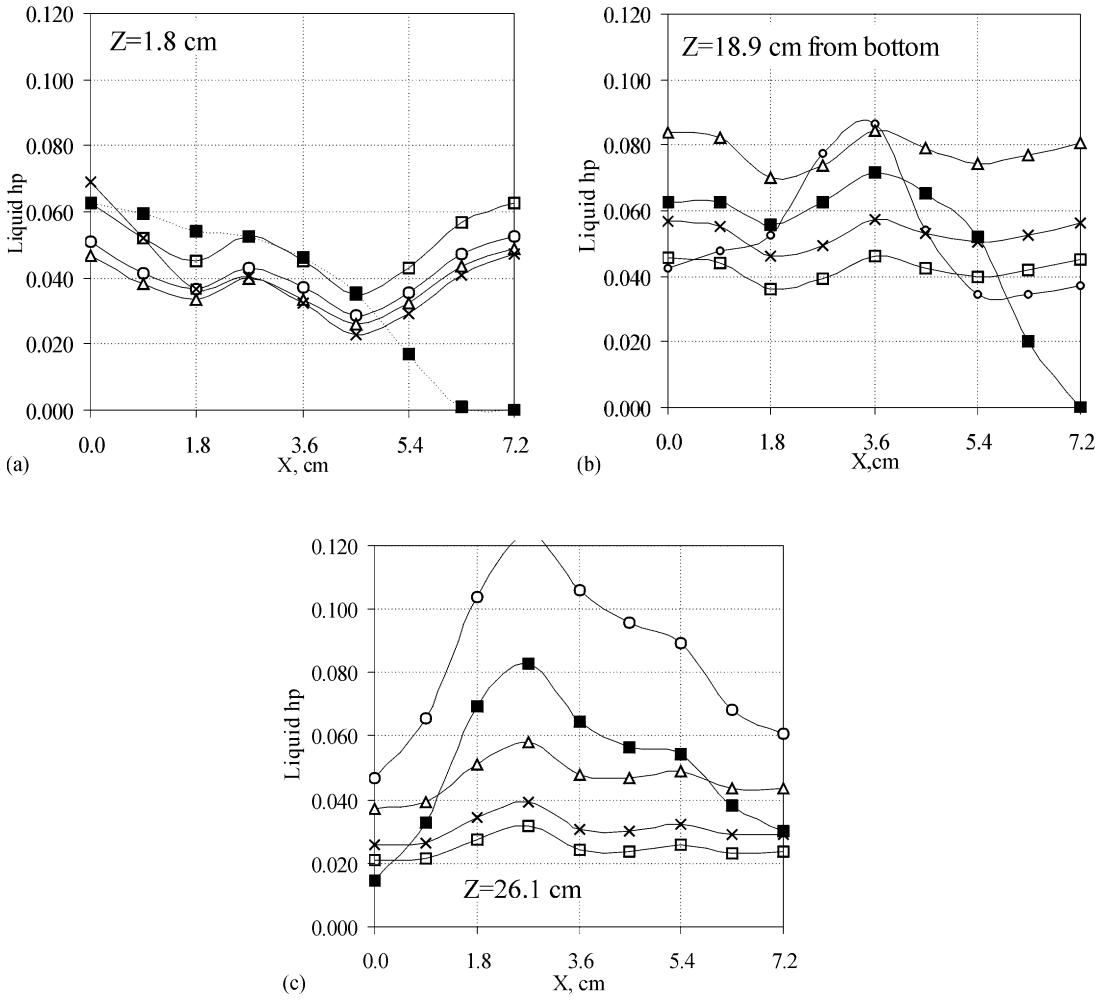

Fig. 5. Comparison of cross-sectional liquid holdup profiles at different axial locations under steady (filled squares) and unsteady state operation ((a), $Z = 1.8$ cm; (b), $Z = 18.9$ cm; (c), $Z = 26.1$ cm) ((○) 15s; (△) 25s; (×) 40s; (□) 55s).

liquid is seen in zones near the bottom of the reactor (Fig. 4b (right)).

The liquid flow distribution observed in the steady state case was compared with transient simulations carried out with a liquid flow ON time of 15 s and a total cycle time of 60 s (45 s liquid OFF).

Snapshots of liquid flow distribution were taken at several time intervals (t = 15, 25, 40 s from beginning of liquid ON time) (Fig. 4c–e) to compare them with the steady state liquid holdup data obtained in the steady state case (Fig. 4b). Liquid holdup variation over the reactor cross-section is depicted at several axial locations at different times in a typical flow modulation cycle (Fig. 5a–c). These figures clearly demonstrate that unsteady state operation ensures better uniformity in liquid distribution at all locations compared to that observed in steady state operation. This improved distribution, though not perfect, does ensure enhanced liquid supply to all locations not previously possible during steady state (in particular, the bottom zone shown in Fig. 5a). This clearly shows that induced flow modulation results in better liquid spreading and even distribution of liquid over the entire cross-section at each axial location at some point in time in the cycle. This also indicates that although the average liquid holdup at each location may not exceed the steady state holdup, the reactor performance may still be enhanced due to higher than steady state holdup for a sub-interval of the entire cycle. This time interval of enhanced liquid supply can allow exchange of liquid reactants and products with the stagnant liquid and with the catalyst pellets present in any particular zone. Another observation that can be made from Fig. 4e is that for some time interval, all zones in the reactor become almost completely devoid of liquid, and can allow enhanced access of the gaseous reactant to externally dry catalyst during this time interval. Temperature rise and internal drying of catalyst and faster gas phase reaction may also occur in this interval, which can be quenched by the liquid in the next cycle.

The above simulation demonstrates the possibility of controlled rate enhancement due to induced flow modulation. It also facilitates our understanding and visualization of the phenomena occurring in the reactor. It confirms the reasons behind improved unsteady state performance observed experimentally and simulated in the reaction transport models [26,39–42]. It seems that upon scale up large reactors operated with flow modulation should perform with the same enhancement over steady state operation as seen in the scaled down version.

5. Concluding remarks

CFD flow modeling of bench-scale packed beds provides valuable information for improving experimental protocol and data interpretation of scale down reactors. To evaluate the impact of the flow distribution on the performance of packed bed reactors for a given kinetics, a mixing-cell network model has been proposed as sequential model in which the k-fluid CFD model results are used as input information on the multiphase flow field [43]. The combination of this work with the developed mixing-cell network model allows one to evaluate the performance of bench-scale packed bed reactor more realistically, even for the system of complex reaction kinetics. Experimental validation of this work should be possible by using advanced non-invasive tomgraphic techniques such as MRI and high-resolution CT.

Acknowledgements

The authors would like to acknowledge the support provided by the industrial sponsors of the CREL.

References

[1] S.T. Sie, R. Krishna, Rev. Chem. Eng. 14 (1998) 203–252.
[2] J.W. Le Nobel, J.H. Choufour, Proceedings of the Fifth World Petroleum Congress Section III, 5th WPC Inc., New York, 1959, pp. 233–243.
[3] H. Gieman, Appl. Catal. 43 (1988) 277–286.
[4] M. de Wind, F.L. Plantenga, J.J.L. Heinerman, H.W. Homan Free, Appl. Catal. 43 (1988) 239–252.
[5] R. Krishna, S.T. Sie, Chem. Eng. Sci. 49 (1994) 4029.
[6] M.P. Dudukovic, F. Larachi, P.L. Mills, Chem. Eng. Sci. 54 (1999) 1975–1995.
[7] D.E. Mears, Chem. Eng. Sci. 26 (1971) 1361–1366.
[8] D. Tasmatsoulis, N. Papayannakos, Chem. Eng. Sci. 49 (1994) 523–529.
[9] J. van Klinken, R.H. van Dongen, Chem. Eng. Sci. 35 (1980) 59–66.
[10] M.H. Al-Dahhan, M.P. Dudukovic, AIChE J. 42 (1996) 2594–2606.
[11] J.J. Lerou, G.F. Froment, Chem. Eng. Sci. 32 (1977) 853–861.

[12] J.L. Stephenson, W.E. Stewart, Chem. Eng. Sci. 53 (1986) 1375.
[13] A.J. Sederman, M.L. Johns, A.S. Bramley, P. Alexander, L.F. Gladden, Chem. Eng. Sci. 48 (1997) 2239–2250.
[14] P.G. Lutran, K.M. Ng, E.P. Delikat, Ind. Eng. Chem. Res. 30 (1991) 951.
[15] L.F. Gladden, Chem. Eng. Sci. 49 (1994) 3339–3408.
[16] J. Chaouki, F. Larachi, M.P. Dudukovic, Non-Invasive Monitoring of Multiphase Flows, Elsevier, Amsterdam, 1997.
[17] N. Reinecke, G. Petritsch, D. Schmitz, D. Mewes, Chem. Eng. Technol. 21 (1998) 7.
[18] V. Stanek, Fixed Bed Operations: Flow Distribution and Efficiency, Ellis Horwood, Chichester, UK, 1994.
[19] S.P. Zimmerman, K.M. Ng, Chem. Eng. Sci. 41 (1986) 861.
[20] M. Crine, P. Marchot, G.A. L'Homme, Comp. Chen Eng. 3 (1979) 515.
[21] G. Christensen, S.J. McGovern, S. Sundaresan, AIChE J. 32 (1986) 1677–1689.
[22] R.A. Holub, Ph.D. Thesis, Washington University in St. Louis, MO, 1990.
[23] Y. Jiang, M.R. Khadilkar, M.H. Al-Dahhan, M.P. Dudukovic, Chem. Eng. Sci. 54 (1999) 2109–2119.
[24] Y. Jiang, M.R. Khadilkar, M.H. Al-Dahhan, M.P. Dudukovic, Chem. Eng. Sci. 55 (2000) 1829–1844.
[25] S.A. Logtenberg, A.G. Dixon, Chem. Eng. Process. 37 (1998) 7–21.
[26] M.R. Khadilkar, M.H. Al-Dahhan, M.P. Dudukovic, Chem. Eng. Sci. 54 (1999) 2585–2595.
[27] R.F. Benenati, C.B. Brosilow, AIChE J. 8 (1962) 359.
[28] W.S. Jodrey, E.M. Tory, Power Tech. 30 (1981) 111–118.
[29] J.G.H. Borkink, C.G. van de Watering, K.R. Westerterp, Trans. IChemE A 70 (1992) 610–619.
[30] B.A. Kashiwa, N.T. Padial, R.M. Rauenzahn, W.B. vander Heyden, in: Proceedings of the ASME Symposium on Numerical Methods for Multiphase Flows, Lake Tahoe, Nevada, 1994.
[31] Y. Jiang, M.R. Khadilkar, M.H. Al-Dahhan, M.P. Dudukovic, AIChE J., (2001) in press.
[32] R.A. Holub, M.P. Dudukovic, P.A. Ramachandran, Chem. Eng. Sci. 47 (1992) 2343–2348.
[33] A. Attou, C. Boyer, G. Ferschneider, Chem. Eng. Sci. 54 (1999) 785–802.
[34] K.A. Grosser, R.G. Carbonell, S. Sundaresan, AIChE J. 34 (1988) 1850.
[35] M.H. Muthanna, M.P. Dudukovic, Chem. Eng. Sci. 50 (1995) 2377–2389.
[36] S. Highfill, M.Sc. Thesis, Washington University in St. Louis, MO, 1998.
[37] M.A. Latifi, N. Midoux, A. Storck, Chem. Eng. Sci. 44 (1989) 2501.
[38] M.H. Al-Dahhan, M.R. Khadilkar, Y. Wu, M.P. Dudukovic, Ind. Eng. Chem. Res. 37 (1998) 793–798.
[39] R. Lange, J. Hanika, D. Strsdiotto, R.R. Hudgins, P.L. Silveston, Chem. Eng. Sci. 49 (1994) 5615.
[40] A. Castellari, P.M. Haure, AIChE J. 41 (1995) 1593–1597.
[41] M.R. Khadilkar, Ph.D. Thesis, Washington University, St. Louis, MO, 1998.
[42] P.L. Silveston, Unsteady State Processes in Catalysis. In: Yh. Sh. Matros (Ed.), Proc. of the Int. Conf., Novosibirsk. 1990, pp. 217–232.
[43] Y. Jiang, Ph.D. Thesis, Washington University, St. Louis, MO, 2000.